# Supporting Information

**Thiol-reactive Passerini-methacrylates and Polymorphic Surface Functional Soft Matter Nanoparticles via Ethanolic RAFT Dispersion Polymerization and Post-synthesis Modification**

Yiwen Pei, Janina-Miriam Noy, Peter J. Roth, and Andrew B. Lowe*

School of Chemical Engineering, Centre for Advanced Macromolecular Design, UNSW Australia, University of New South Wales, Kensington, Sydney, NSW 2052, Australia.

profandrewblowe@gmail.com

## Experimental Section

**Materials.** All reagents were purchased from the Sigma-Aldrich Chemical Company and used as received unless otherwise noted. 2,2'-Azobis(isobutyronitrile) (AIBN) was purified by two recrystallizations from methanol. 2-(Dimethylamino)ethyl methacrylate (DMAEMA), 3-phenylpropyl methacrylate (PPMA) was passed through a basic $Al_2O_3$ column to remove inhibitors prior to use. Novel pentafluorophenyl (PFP)-containing methacrylic monomers, 2-(cyclohexylamino)-2-oxo-1-(perfluorophenyl)ethyl methacrylate (CyAFPEMA), 2-((2-ethoxy-2-oxoethyl)amino)-2-oxo-1-(perfluorophenyl) ethyl methacrylate (EAFPEMA) and 2-(*tert*-butylamino)-2-oxo-1-(perfluorophenyl)ethyl

methacrylate (*t*BAFPEMA), were prepared via the Passerini reaction as described recently by Roth *et al.*[1,2] and 4-Cyanopentanoic acid dithiobenzoate (CPADB) was prepared according to a procedure described elsewhere.[3]

**Copolymer Characterizations**

Size exclusion chromatography (SEC) was performed on a Shimadzu system with four phenogel columns ($10^2$, $10^3$, $10^4$, $10^6$ Å pore size) in *N, N*-dimethylacetamide (DMAc) operating at a flow rate of 1 mL $min^{-1}$ at 40 °C using a RID-10A refractive index detector. Chromatograms were analyzed by Cirrus SEC software version 3.0. The system was calibrated with a series of narrow molecular weight distribution polystyrene standards with molecular weights ranging from 0.58-1820 kg $mol^{-1}$.

Transmission electron microscopy (TEM) imaging was conducted at 100 kV on a JEOL1400 TEM instrument. To prepare TEM samples, 5.0 μL of a dilute copolymer solution (0.7 w/w %) was deposited onto a copper grid (ProSciTech), stained with uranyl acetate (0.2 w/w % in water), and dried under ambient conditions.

DLS measurements were performed using a Malvern Instrument Zetasizer Nano Series instrument equipped with a 4 mW He-Ne laser operating at 633 nm and an avalanche photodiode (APD) detector. The scattered light was detected at an angle of 173°. For sample preparation, 0.1 mL of the parent RAFTDP solution was diluted with 2.9 mL of ethanol and the solution then stirred for 5 min prior to double filtration through 0.45 μm nylon filters.

Fourier transform infrared (FTIR) spectroscopy was conducted on a Bruker IFS 66/S

instrument under attenuated total reflectance (ATR) and the results were analyzed utilizing OPUS software version 4.0.

NMR characterization analyses were conducted using a Bruker Avance III 300 spectrometer (300.13 MHz for $^{1}$H nuclei and 282 MHz for $^{19}$F nuclei). The internal solvent signal of $CDCl_3$ was utilized for reference (δ = 7.26 ppm). The number average molecular weight, $\bar{M}_{n,NMR}$, was calculated based on a full conversion of Passerini methacrylate (confirmed by $^{19}$F NMR) and the average degree of polymerization, $\bar{X}_n$ of PDMAEMA in RAFT macroCTAs. $\bar{X}_n$ of PDMAEMA was estimated based on the integral values of the signals at δ = 4.06 ppm and 7.30-7.90 ppm, as shown in eqn (1).

$$\bar{X}n\ (PDMAEMA) = \frac{5 \times\ I\ (4.60\ ppm)}{2\ \times\ I\ (7.30 - 7.90\ ppm)} \quad (1)$$

The absolute molecular weight, $\bar{M}_{n,NMR}$, and $\bar{X}_n$ of block copolymers were calculated based on $\bar{X}_n$ of the PDMAEMA-Passerini macro-CTA and the integration ratio of the signal at δ = 7.10-7.50 ppm ($I_{7.10\text{-}7.50ppm}$, aryl protons of PPPMA) and those at 2.30 ppm ($I_{2.30ppm}$, methyl protons of PDMAEMA in RAFT macro-CTA), as shown in Figure 2-4 and eqn (2). We also compared the integration ratio between the methylene protons of the PDMAEMA block (δ = 4.20 ppm) and the methylene protons of the PPPMA block (δ = 3.90 ppm) to obtain accurate polymer compositions.

$$\bar{X}n\ (PPPMA) = \frac{6 \times\ I\ (7.70 - 7.50\ ppm)}{5\ \times\ I\ (2.30\ ppm)} \bar{X}n\ (PDMAEMA) \quad (2)$$

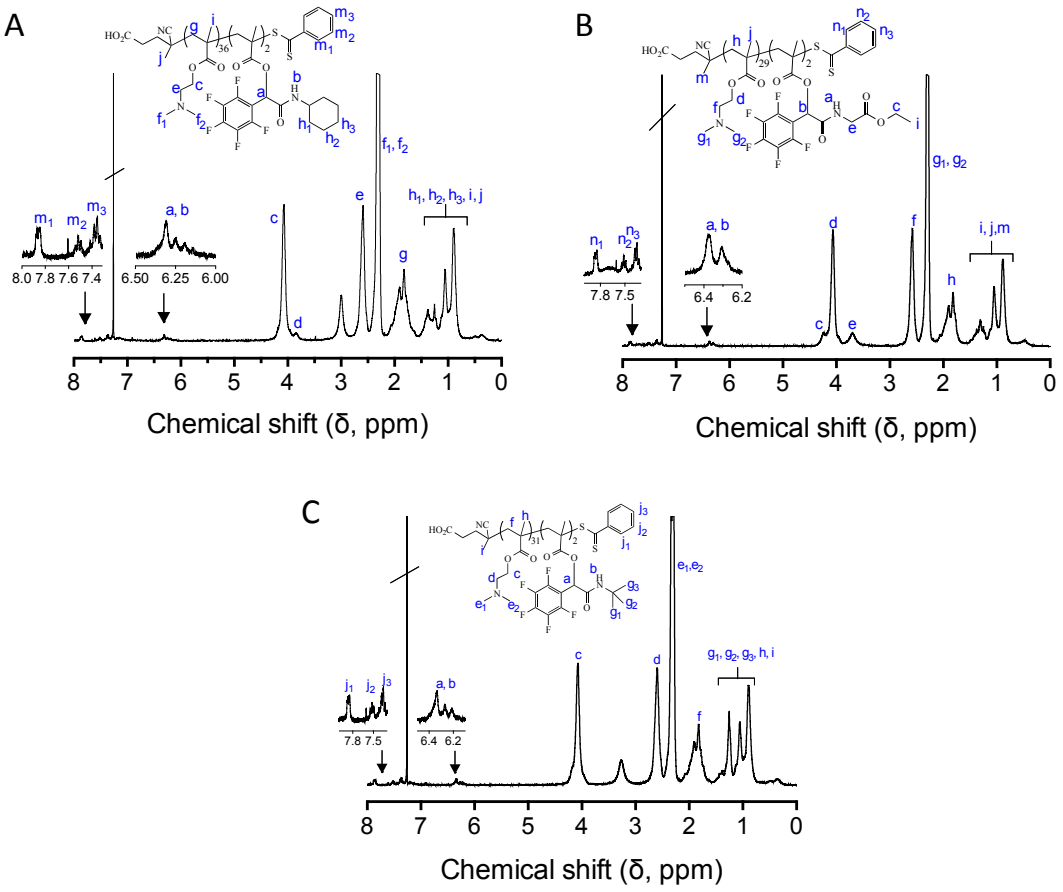


**Figure S1.** $^{1}$H NMR spectra of DMAEMA-Passerini macro-CTAs (A) P(DMAEMA$_{36}$-*co*-CyAFPEMA$_2$), (B) P(DMAEMA$_{29}$-*co*-EAFPEMA$_2$) and (C) P(DMAEMA$_{31}$-*co*-*t*BAFPEMA$_2$), recorded in $CDCl_3$, with peak assignments. Inset is an expanded region highlighting the presence of the phenyldithioester end group, benzylic and NH hydrogen.

A

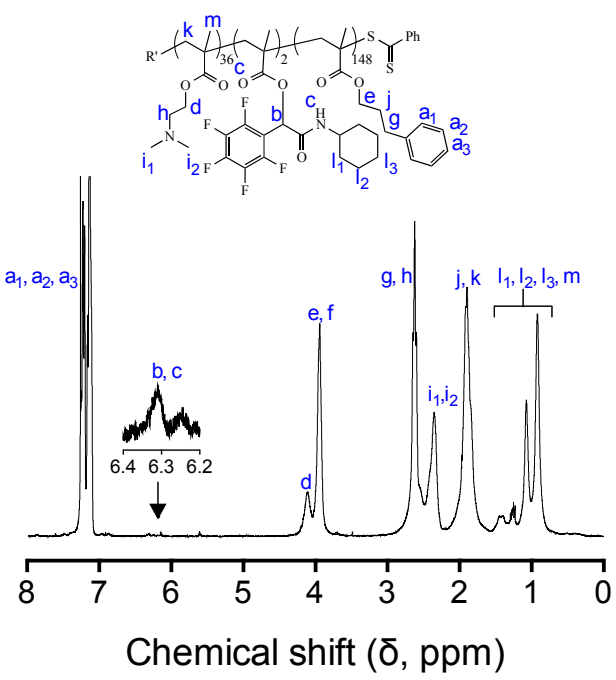


B

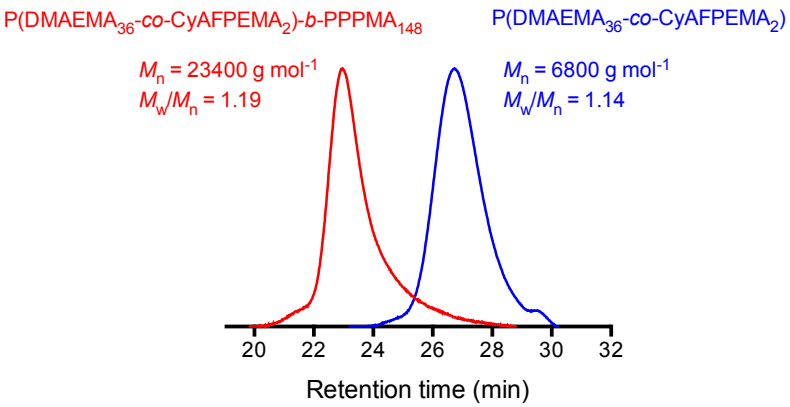


**Figure S2.** (A) $^{1}$H NMR spectrum of PFP-functional copolymer, P(DMAEMA$_{36}$-*co*-CyAFPEMA$_2$)-*b*-PPPMA$_{148}$ and (B) representative size exclusion chromatograms of the resulting polymer obtained by RAFTDP.

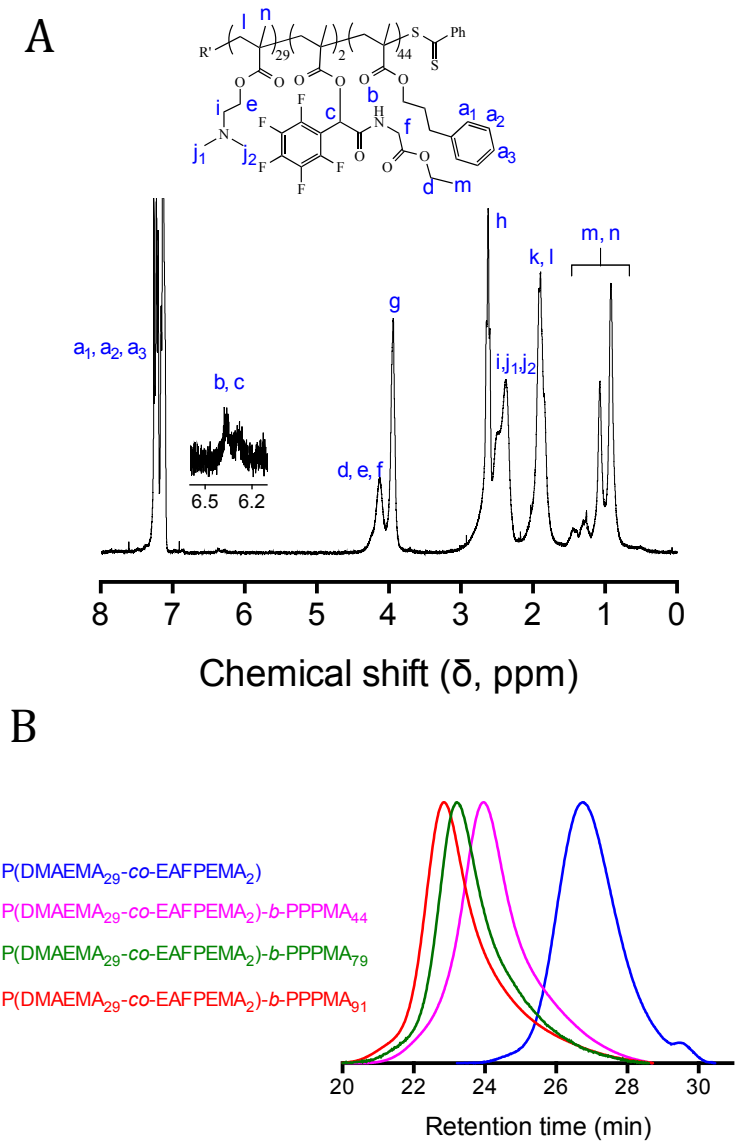


**Figure S3.** (A) $^{1}$H NMR spectrum of PFP-functional copolymer, P(DMAEMA$_{29}$-*co*-EAFPEMA$_2$)-*b*-PPPMA$_{44}$ and (B) representative size exclusion chromatograms of the resulting polymers obtained by RAFTDP.

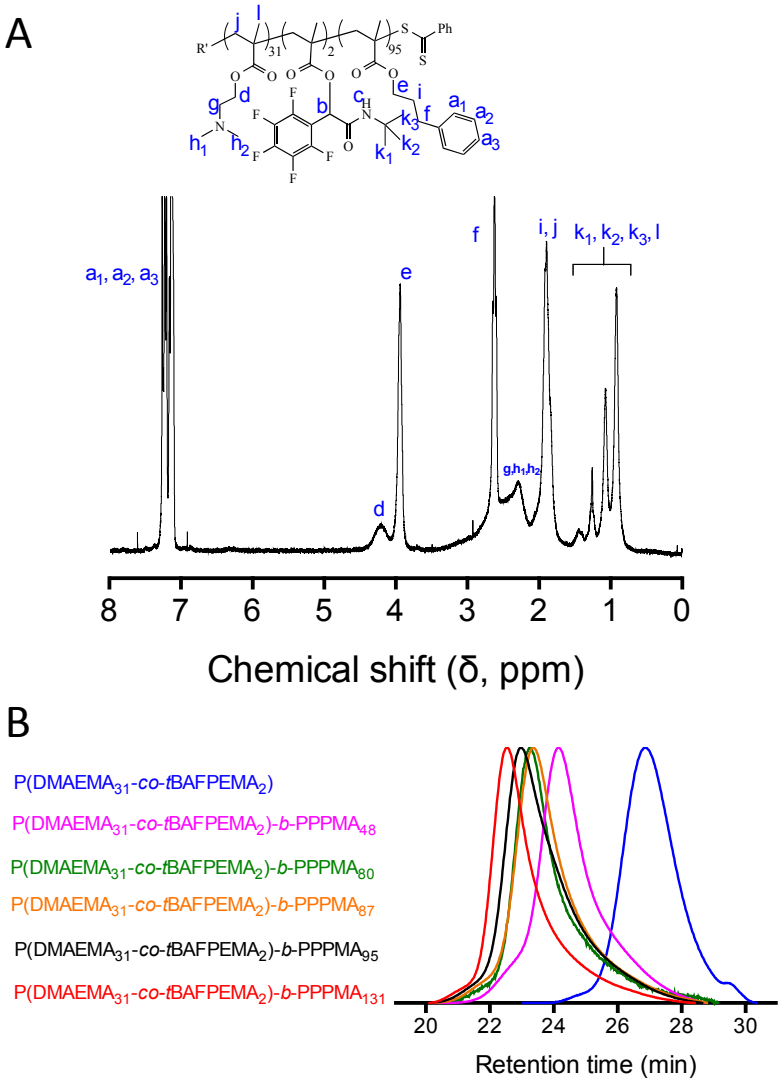


**Figure S4.** (A) $^{1}$H NMR spectrum of PFP-functional copolymer, P(DMAEMA$_{31}$-*co*-*t*BAFPEMA$_2$)-*b*-PPPMA$_{95}$ and (B) representative size exclusion chromatograms of the resulting polymers obtained by RAFTDP.

**Table S1. Summary of RAFTDP syntheses with macro-CTAs and PPMA as a comonomer in EtOH at 21 wt% and 70 °C. The NMR-determined average degree of polymerization ($\bar{X}_n$) of the PPMA block and absolute molecular weight are given along with the SEC-measured $\bar{M}_n$ and dispersities, TEM morphology, TEM-measured diameter and DLS-measured hydrodynamic diameter and polydispersities.**

| Macro-CTA | Conv. % | PPMA $X_n$ | NMR MW[a] | SEC $\bar{M}_n$[b] | SEC $Đ_M$[b] | TEM morp.[c] | TEM $D$[d] | DLS $D_h$[e] | DLS PDI |
|---|---|---|---|---|---|---|---|---|---|
| P(DMAEMA$_{36}$-*co*-CyAFPEMA$_2$) | 95 | 148 | 36,900 | 23,400 | 1.19 | S+W | 54.5 | 141.8 | 0.21 |
| P(DMAEMA$_{29}$-*co*-EAFPEMA$_2$) | 96 | 44 | 14,300 | 17,300 | 1.19 | S | 41.2 | 53.4 | 0.17 |
| P(DMAEMA$_{29}$-*co*-EAFPEMA$_2$) | 95 | 79 | 21,400 | 21,200 | 1.19 | S+W | 45.6 | 81.4 | 0.17 |
| P(DMAEMA$_{29}$-*co*-EAFPEMA$_2$) | 92 | 91 | 23,900 | 22,900 | 1.24 | W+V | 234.3 | 215.0 | 0.21 |
| P(DMAEMA$_{31}$-*co*-*t*BAFPEMA$_2$) | 91 | 48 | 15,700 | 16,200 | 1.18 | S | 47.0 | 45.8 | 0.18 |
| P(DMAEMA$_{31}$-*co*-*t*BAFPEMA$_2$) | 95 | 80 | 22,300 | 19,600 | 1.23 | S+W | 53.2 | 137.1 | 0.19 |
| P(DMAEMA$_{31}$-*co*-*t*BAFPEMA$_2$) | 95 | 87 | 23,700 | 19,900 | 1.21 | S+W | 54.9 | 190.1 | 0.19 |
| P(DMAEMA$_{31}$-*co*-*t*BAFPEMA$_2$) | 92 | 95 | 25,200 | 21,300 | 1.23 | W | 55.1 | 223.4 | 0.19 |
| P(DMAEMA$_{31}$-*co*-*t*BAFPEMA$_2$) | 87 | 131 | 32,700 | 25,800 | 1.21 | W+V | 275.3 | 230.7 | 0.79 |

[a] As determined by end group analysis; [b] as measured in THF on a system calibrated with polystyrene standards; [c] S = spheres, W = worms, V = vesicles; [d] TEM-measured nanoparticle diameter in nm; [e] hydrodynamic diameter in nm.

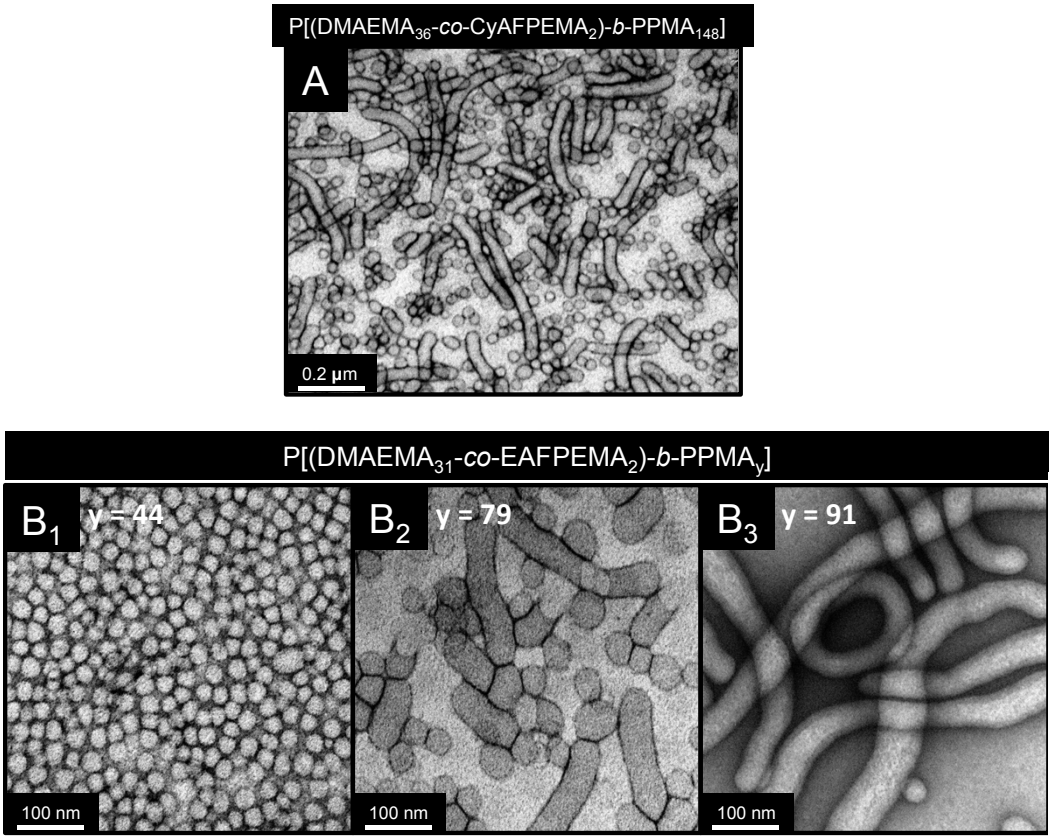


**Figure S5.** Representative TEM images obtained for (A) P(DMAEMA$_{36}$-*co*-CyAFPEMA$_2$)-*b*-PPPMA$_{148}$ and (B) P(DMAEMA$_{29}$-*co*-EAFPEMA$_2$)-*b*-PPPMA$_y$ copolymer nanoparticles synthesized at a total solids concentration of 21 wt% using RAFT dispersion polymerization in ethanol at 70 °C.

**Table S2.** Summary of thiol-*p*-fluoro postpolymerization modification performed in ethanol at 50 °C overnight (up to 2 days for the reaction with worm-like copolymers[c]). Complete substitution was confirmed for all reactions by $^{19}F$ NMR spectroscopy.

| Entry | PFP-Functional Nano-Objects | Thiol | Base | Thiol/PFP | Thiol/Base |
|---|---|---|---|---|---|
| 1[a] | p[(DMAEMA$_{29}$-*co*-EAFPEMA$_2$)-PPMA$_{44}$] | 2-mercaptoethanol | DBU | 5 | 1 |
| 2[a] | p[(DMAEMA$_{29}$-*co*-EAFPEMA$_2$)-PPMA$_{44}$] | cysteamine hydrochloride | DBU | 20 | 0.5 |
| 3[a] | p[(DMAEMA$_{31}$-*co*-*t*BAFPEMA$_2$)-PPMA$_{48}$] | 1-thio-β-D-glucose tetraacetate | $Et_3N$ | 20 | 1 |
| 4[b] | p[(DMAEMA$_{31}$-*co*-*t*BAFPEMA$_2$)-PPMA$_{80}$] | Captopril | DBU | 5 | 0.5 |
| 5[b] | p[(DMAEMA$_{31}$-*co*-*t*BAFPEMA$_2$)-PPMA$_{80}$] | thiophenol | $Et_3N$ | 10 | 1 |
| 6[c] | p[(DMAEMA$_{31}$-*co*-*t*BAFPEMA$_2$)-PPMA$_{95}$] | 1-thio-β-D-glucose tetraacetate | $Et_3N$ | 50 | 1 |

[a] Pure sphere phase; [b] Mixed spheres/worms phase; [c] Pure worm phase.

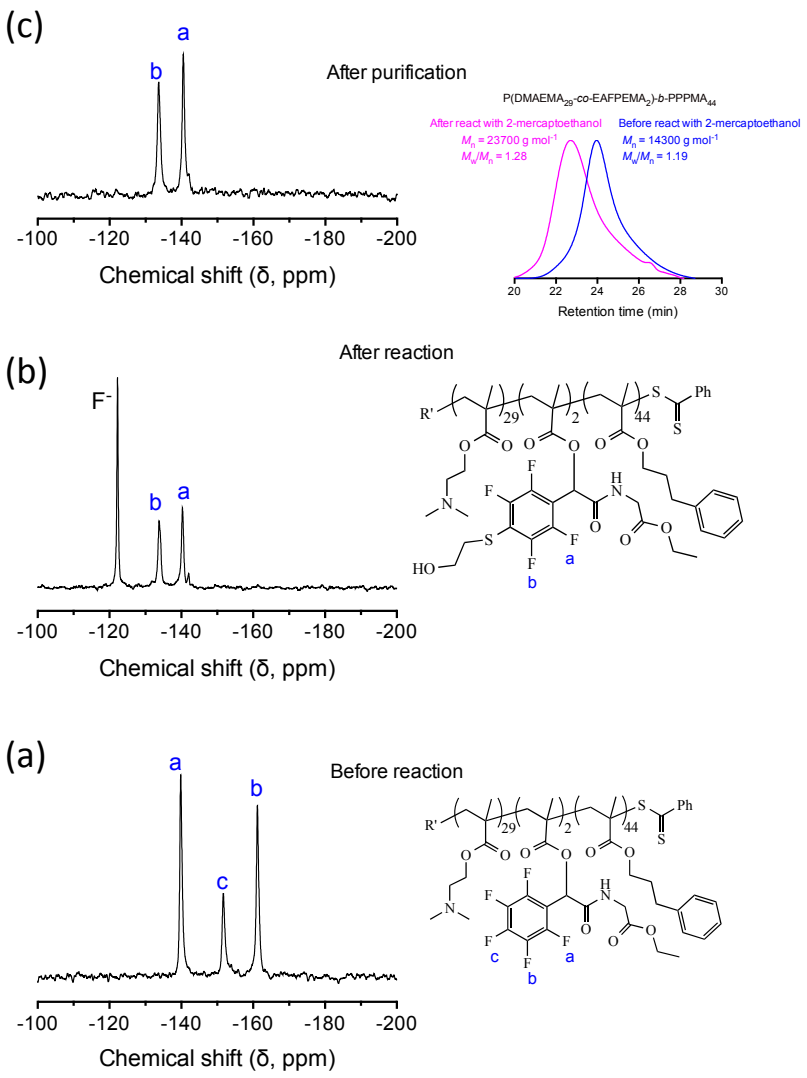


**Figure S6.** (a) $^{19}F$ NMR spectra of the P[(DMAEMA$_{29}$-*co*-EAFPEMA$_2$)-*b*-PPMA$_{44}$] exhibiting *ortho*, *meta* and *para* signals associated with the PFP functionality in the Passerini repeat units; (b) after reaction of the spherical nanoparticles with 2-mercaptoethanol, and (c) after purification of the surface modified nano-spheres, with SEC traces before and after reaction shown inset.

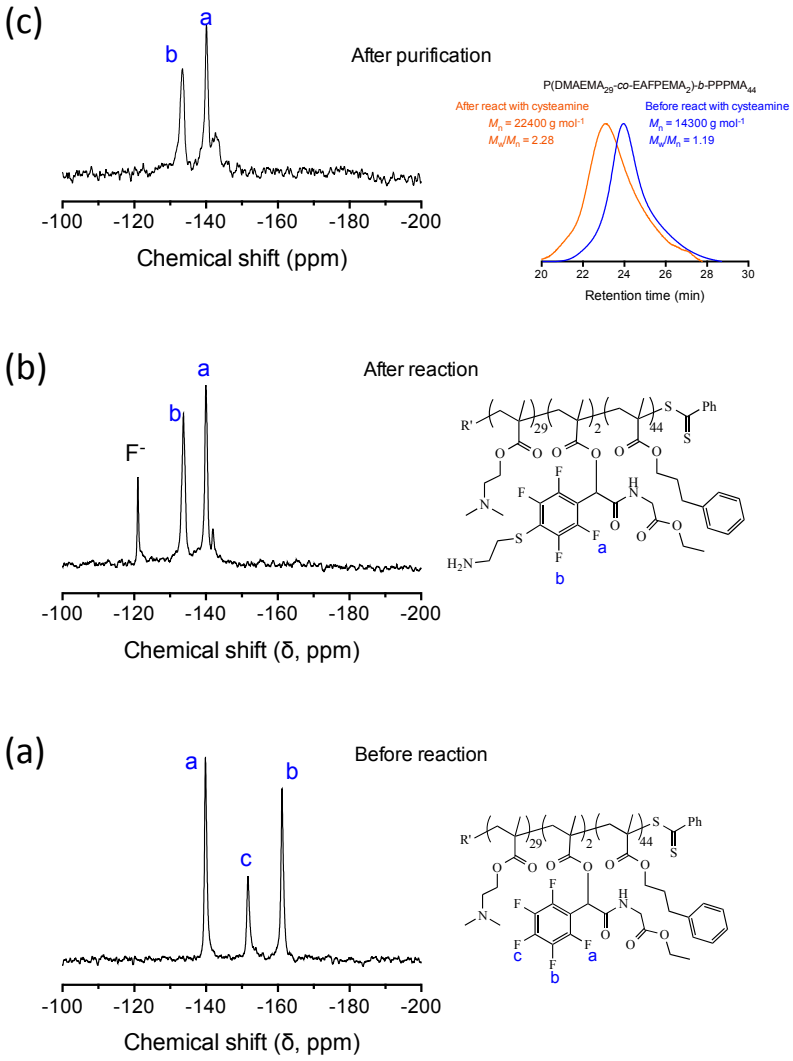


**Figure S7.** (a) $^{19}F$ NMR spectra of the P[(DMAEMA$_{29}$-*co*-EAFPEMA$_2$)-*b*-PPMA$_{44}$] exhibiting *ortho*, *meta* and *para* signals associated with the PFP functionality in the Passerini repeat units; (b) after reaction of the spherical nanoparticles with cysteamine hydrochloride, and (c) after purification of the surface modified nano-spheres, with SEC traces before and after reaction shown inset.

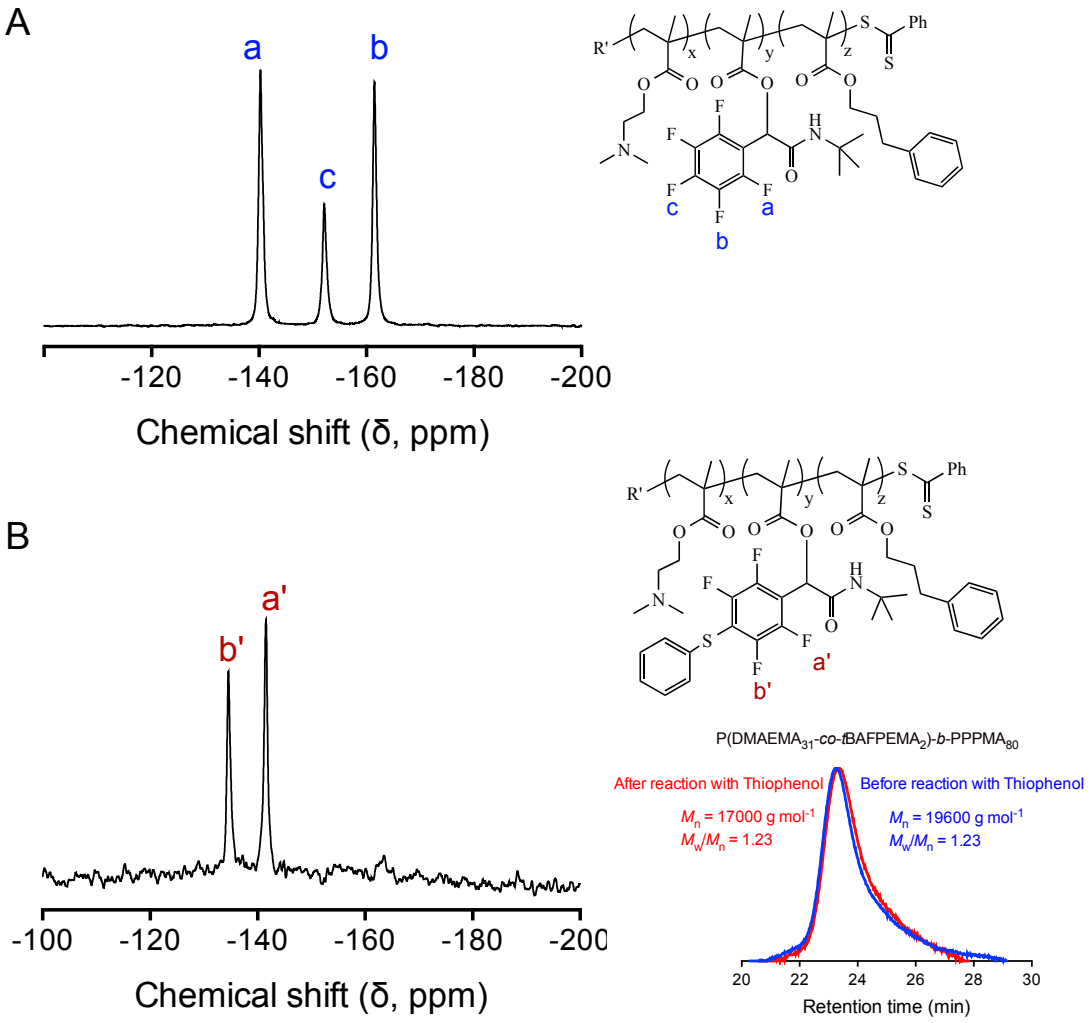


**Figure S8.** $^{19}F$ NMR spectra of the (A) unmodified and (B) surface-modified mixed phased sphere/worm nano-objects by reacting P[(DMAEMA$_{31}$-*co*-*t*BAFPEMA$_2$)-*b*-PPMA$_{80}$] with thiophenol, recorded in $CDCl_3$, with peak assignments, with SEC trace before and after reaction shown inset.

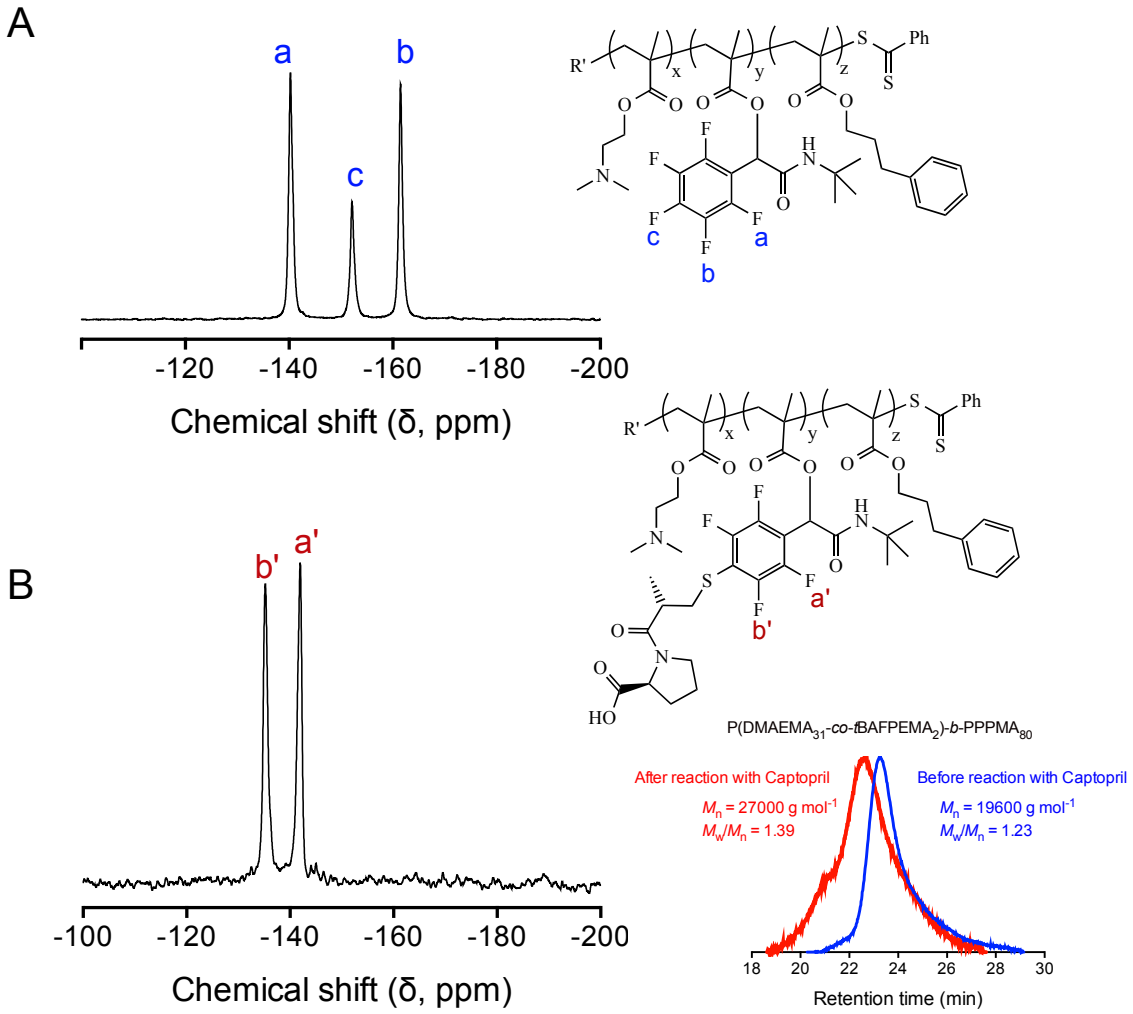


**Figure S9.** $^{19}F$ NMR spectra of the (A) unmodified and (B) surface-modified mixed phased nano-objects by reacting P[(DMAEMA$_{31}$-*co*-*t*BAFPEMA$_2$)-*b*-PPMA$_{80}$] with Captopril, recorded in $CDCl_3$, with peak assignments, with SEC trace before and after reaction shown inset.

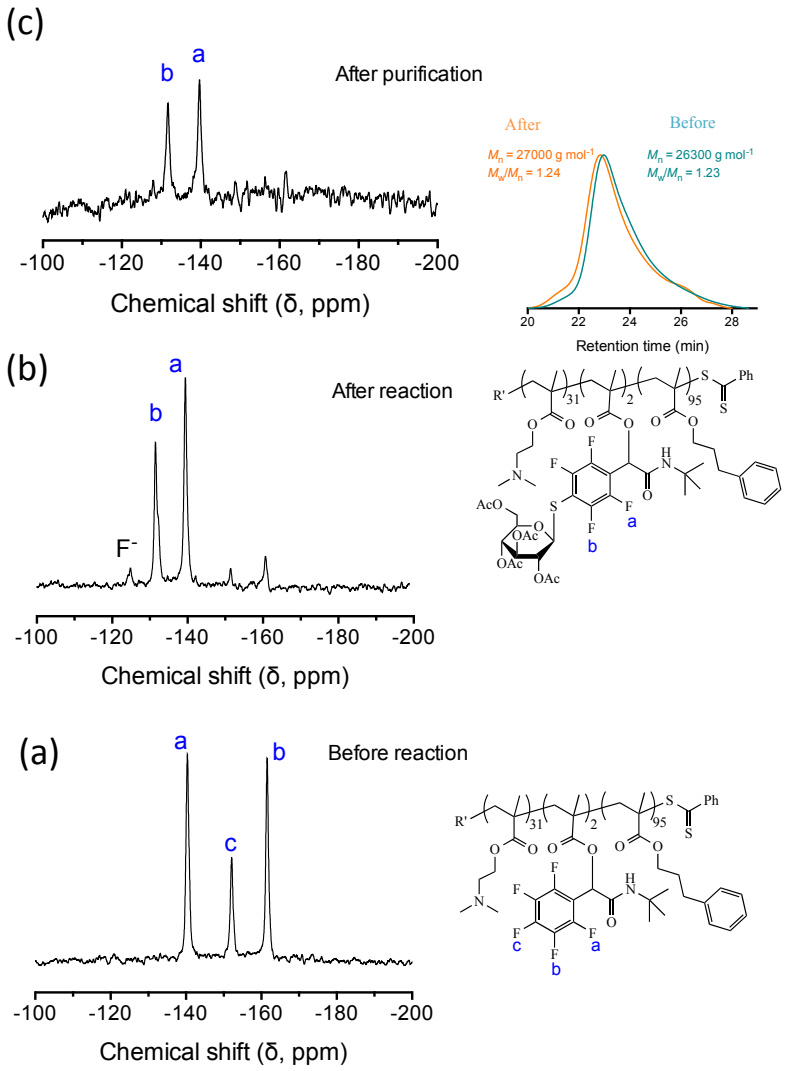


**Figure S10.** (a) $^{19}$F NMR spectra of the P[(DMAEMA$_{31}$-*co*-*t*BAFPEMA$_2$)-*b*-PPMA$_{95}$] exhibiting *ortho*, *meta* and *para* signals associated with the PFP functionality in the Passerini repeat units; (b) after reaction of the spherical nanoparticles with 1-thio-β-D-glucose tetraacetate, and (c) after purification of the surface-functional worm-like copolymers, with SEC traces before and after reaction shown inset.

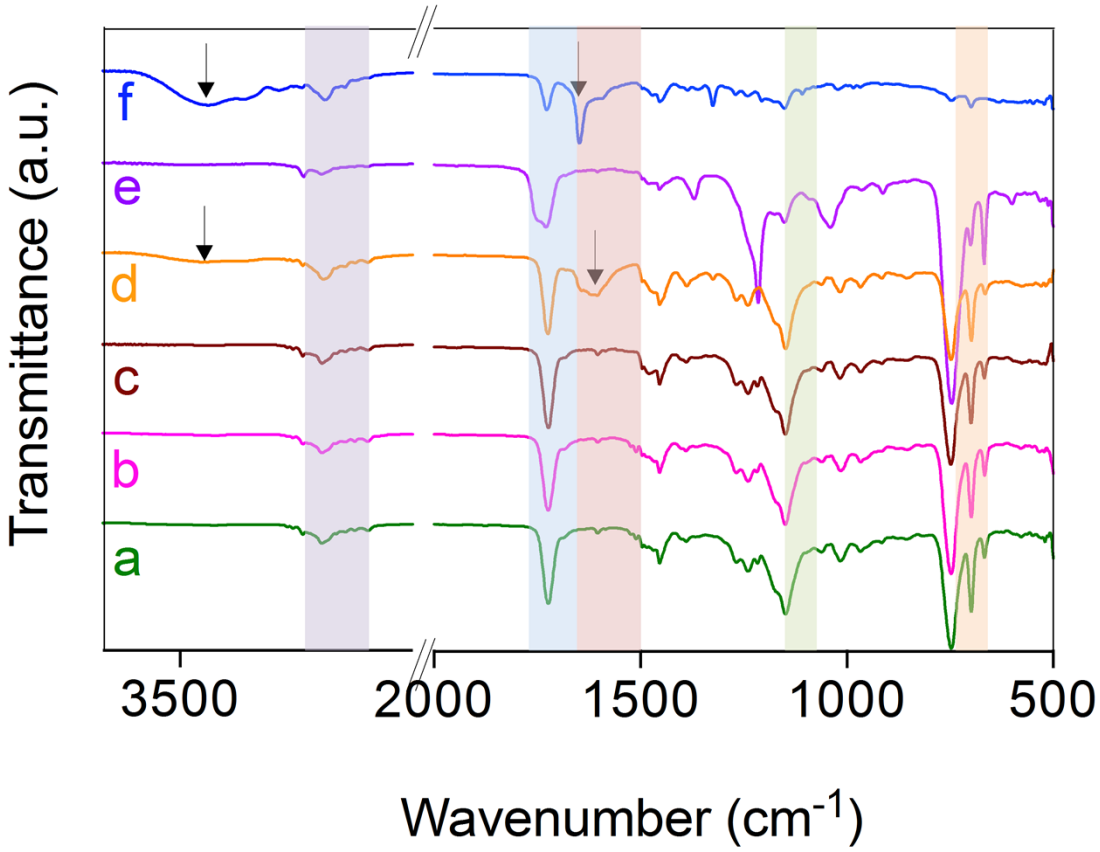


**Figure S11.** FT-IR spectra of unmodified block copolymer, P[(DMAEMA$_{31}$-*co*-*t*BAFPEMA$_2$)-*b*-PPMA$_{95}$] (**a**, green) and surface modified nano-objects by reaction with 2-mercaptoethanol **(b**, pink), thiophenol (**c**, brown), Captopril (**d**, orange), 1-thio-β-D-glucose tetraacetate (**e**, purple), cysteamine hydrochloride (**f**, blue). The occurrence of amidation in the cysteamine-modified copolymer nanoparticles is evident from the disappearance of distinctive ester band (C=O stretch at ~1730 cm$^{-1}$) and clear appearance of the amide bands at ~3290 (N-H stretch), ~1640 (amide C=O stretching) and ~1530 cm$^{-1}$ (N-H bend).

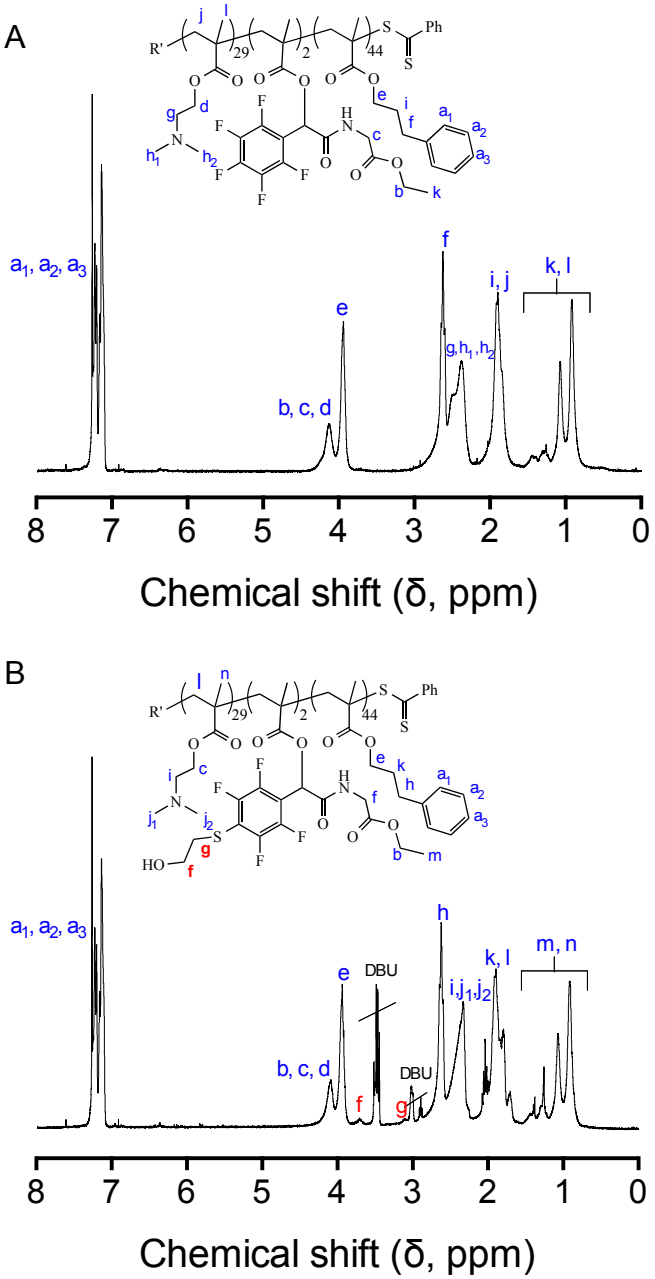


**Figure S12.** $^{1}$H NMR spectra of (A) the unmodified and (B) surface-modified spherical nano-objects by reacting P[(DMAEMA$_{29}$-*co*-EAFPEMA$_{2}$)-*b*-PPMA$_{44}$] with 2-mercaptoethanol, recorded in $CDCl_3$, with peak assignments.

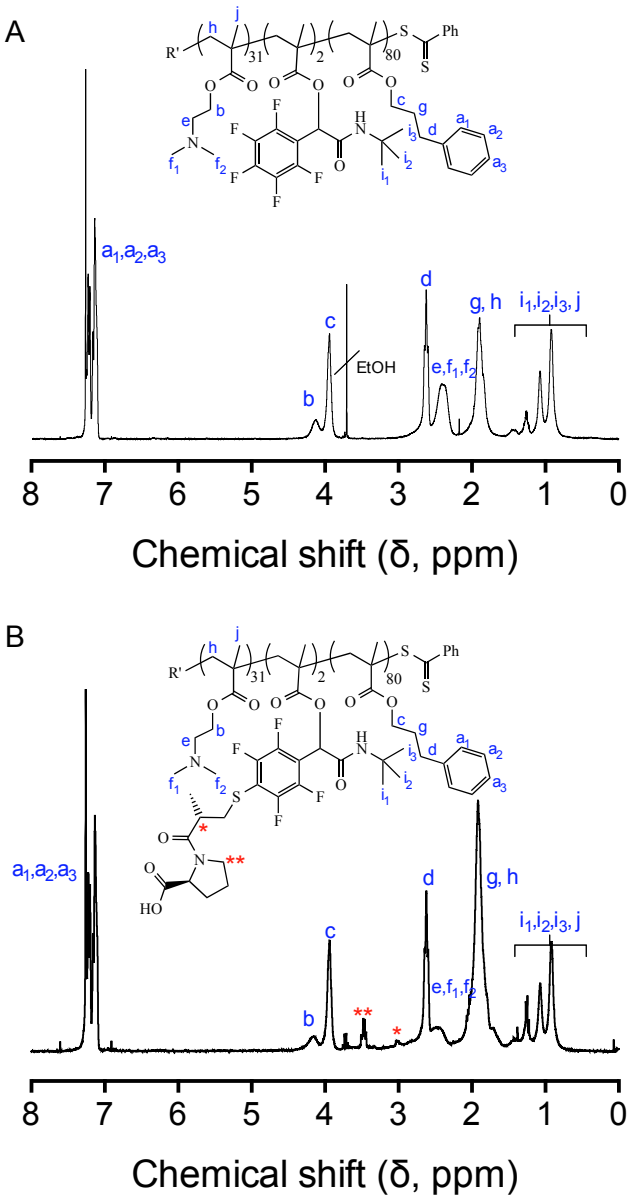


**Figure S13.** $^{1}$H NMR spectra of (A) the unmodified and (B) surface-modified mixed phased nano-objects by reacting P[(DMAEMA$_{31}$-*co*-*t*BAFPEMA$_{2}$)-*b*-PPMA$_{80}$] with Captopril, recorded in $CDCl_3$, with peak assignments.

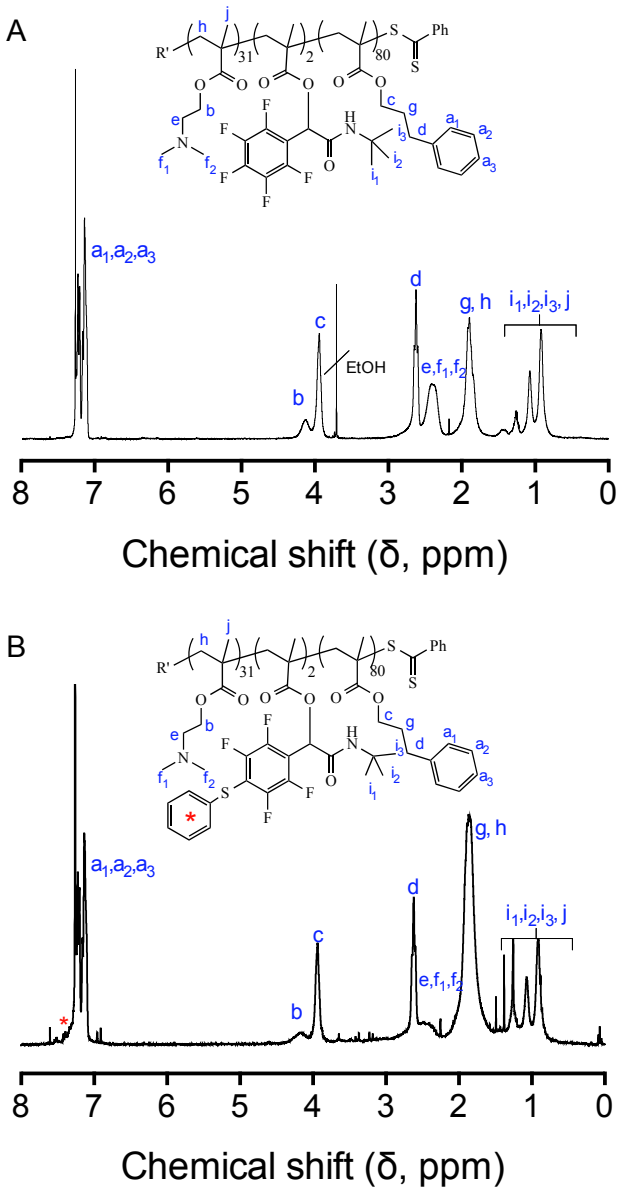


**Figure S14.** $^{1}$H NMR spectra of (A) unmodified and (B) the surface-modified mixed phased nano-objects by reacting P[(DMAEMA$_{31}$-*co*-*t*BAFPEMA$_{2}$)-*b*-PPMA$_{80}$] with thiophenol, recorded in $CDCl_3$, with peak assignments.

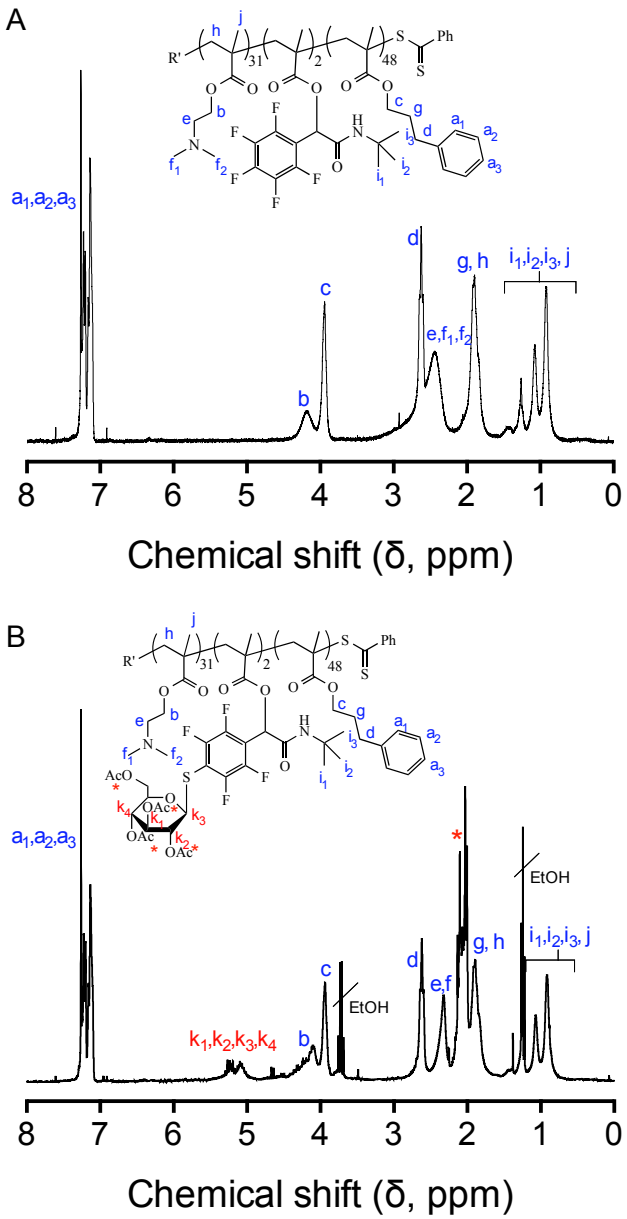


**Figure S15.** $^{1}$H NMR spectra of (A) unmodified and (B) surface-modified spherical nano-objects by reacting P[(DMAEMA$_{31}$-*co*-*t*BAFPEMA$_{2}$)-*b*-PPMA$_{48}$] with 1-thio-β-D-glucose tetraacetate, recorded in $CDCl_3$, with peak assignments.

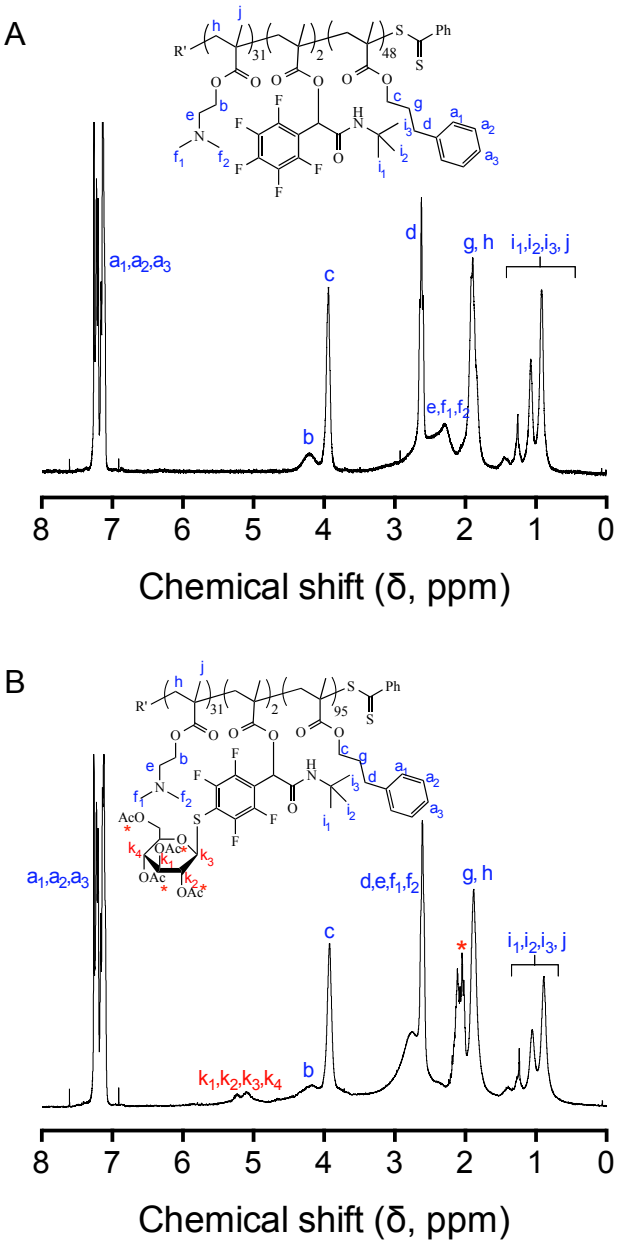


**Figure S16.** $^{1}$H NMR spectra of (A) unmodified and (B) the surface-modified worm-like nano-objects by reacting P[(DMAEMA$_{31}$-*co*-*t*BAFPEMA$_{2}$)-*b*-PPMA$_{95}$] with 1-thio-β-D-glucose tetraacetate, recorded in $CDCl_3$, with peak assignments.

**Reference:**

(1) S. Schmidt, M. Koldevitz, J.-M. Noy, P. J. Roth. *Polym. Chem*., **2014**, DOI: 10.1039/c4py01147c

(2) J.-M. Noy, M. Koldevitz, P. J. Roth. **2014**, DOI: 10.1039/c4py01238k

(3) S. H. Thang, Y. K. Chong, R. T. A. Mayadunne, G. Moad and E. Rizzardo, *Tetrahedron Lett.*, **1999**, 40, 2435–2438